Parallel Solution of Nonlinear Parabolic Problems on Logically Rectangular Grids

A. Arrarás, L. Portero and J.C. Jorge

Departamento de Ingeniería Matemática e Informática
Edificio Las Encinas, Universidad Pública de Navarra
Campus de Arrosadía s/n, 31006 Pamplona (Spain)
{andres.arraras,laura.portero,jcjorge}@unavarra.es[‡]

Abstract. This work deals with the efficient numerical solution of nonlinear transient flow problems posed on two-dimensional porous media of general geometry. We first consider a spatial semidiscretization of such problems by using a cell-centered finite difference scheme on a logically rectangular grid. The resulting nonlinear stiff initial-value problems are then integrated in time by means of a fractional step method, combined with a decomposition of the flow domain into a set of overlapping subdomains and a linearization procedure which involves suitable Taylor expansions. The proposed algorithm reduces the original problem to the solution of several linear systems per time step. Moreover, each one of such systems can be directly decomposed into a set of uncoupled linear subsystems which can be solved in parallel. A numerical example illustrates the unconditionally convergent behaviour of the method in the last section of the paper.

Keywords: Domain Decomposition; Fractional Step Method; Linearly Implicit Method; Logically Rectangular Grid; Nonlinear Parabolic Problem; Support-Operator Method.

1 Introduction

Darcian water flow through non-swelling isothermal soils has been shown to obey Richards' equation [5, 2]. A simplified version of such equation, together with suitable initial and boundary conditions, gives rise to nonlinear parabolic initial-boundary value problems of the following form: Find $\psi : \Omega \times [0,T] \to \mathbb{R}$ such that

$$\begin{cases} \dfrac{\partial \psi(\mathbf{x},t)}{\partial t} = \mathbf{div}(K(\psi)\,\mathbf{grad}\,\psi(\mathbf{x},t)) + g(\psi) + f(\mathbf{x},t), & (\mathbf{x},t) \in \Omega \times (0,T], \\ \psi(\mathbf{x},0) = \psi_0(\mathbf{x}), & \mathbf{x} \in \Omega, \\ \psi(\mathbf{x},t) = \psi_D(\mathbf{x},t), & (\mathbf{x},t) \in \partial\Omega \times (0,T], \end{cases} \tag{1}$$

[‡] This research is partially supported by the Spanish Ministry of Science and Education under Research Project MTM2004-05221 and FPU Grant AP2003-2621 and by Government of Navarre under Research Project CTP-05/R-8.

where $\psi(\mathbf{x},t)$ denotes the pressure head, $K(\psi)$ is a symmetric positive-definite tensor of the form

$$K(\psi) = \begin{pmatrix} K^{11}(\psi) & K^{12}(\psi) \\ K^{12}(\psi) & K^{22}(\psi) \end{pmatrix},$$

which represents nonlinear hydraulic conductivity, $g(\psi)$ is a smooth nonlinear function which may describe, for instance, root water uptake in soil profiles (*cf.* [10]) and $f(\mathbf{x},t)$ is a source/sink term. The flow domain is assumed to be a bounded open set $\Omega \subseteq \mathbb{R}^2$ with boundary $\partial\Omega$, where we have considered Dirichlet boundary conditions $\psi_D(\mathbf{x},t)$.

This paper is devoted to the design of an efficient numerical algorithm for solving problems of type (1). The construction of such scheme is carried out by using a two-stage discretization process (space/time), described in sections 2 and 3. The last section includes a numerical experiment which illustrates the main advantages of the proposed method.

2 Spatial Semidiscretization

The semidiscrete scheme related to (1) is obtained by using a finite difference spatial discretization based on the support-operator method. Such technique, initially developed in [6] and subsequently discussed in [7], provides a methodology for constructing discrete analogs of invariant first-order differential operators which appear in (1) (*i.e.* divergence and gradient). The standard support-operator method was designed for that case in which the self-adjoint operator $\mathbf{div}(K(\mathbf{x})\,\mathbf{grad}\,\psi)$ is linear. However, the nonlinear nature of the conductivity tensor $K(\psi)$ involved in Richards' equation makes it necessary to combine the original technique with a bivariate interpolation method. This section describes the general basis of the discretization scheme, introducing the specifics of our proposal which permit to solve problem (1).

Let us first discretize Ω by means of a logically rectangular grid Ω_h, where h denotes the spatial mesh size. The structure of such grid is indexed as follows: if N_x and N_y are positive integers, then the (i,j)-node is given by the coordinates $(\tilde{x}_{i,j}, \tilde{y}_{i,j})$, for $i \in \{1,2,\ldots,N_x\}$ and $j \in \{1,2,\ldots,N_y\}$. Moreover, the quadrangle defined by the nodes (i,j), $(i+1,j)$, $(i,j+1)$ and $(i+1,j+1)$ is called the (i,j)-cell and its center is given by the coordinates $(x_{i,j}, y_{i,j})$, which can be obtained as

$$\begin{aligned} x_{i,j} &= 0.25\,(\tilde{x}_{i,j} + \tilde{x}_{i+1,j} + \tilde{x}_{i,j+1} + \tilde{x}_{i+1,j+1}), \\ y_{i,j} &= 0.25\,(\tilde{y}_{i,j} + \tilde{y}_{i+1,j} + \tilde{y}_{i,j+1} + \tilde{y}_{i+1,j+1}), \end{aligned}$$

for $i \in \{1,2,\ldots,N_x-1\}$ and $j \in \{1,2,\ldots,N_y-1\}$.

Within this framework, the support-operator method considers cell-centered approximations for scalar functions $\psi(\mathbf{x},t)$, $g(\psi)$ and $f(\mathbf{x},t)$ denoted by $\psi_h(t)$, $g_h(\psi_h)$ and $f_h(t)$, respectively. On the other hand, vector functions $\mathbf{w}(\mathbf{x},t) \equiv (w^x(\mathbf{x},t), w^y(\mathbf{x},t))$ are nodally discretized by means of $\tilde{\mathbf{w}}_h(t) \equiv (\tilde{w}_h^x(t), \tilde{w}_h^y(t))$.

As described in [9], it is natural to use the divergence as the first-order *prime operator* for this approximation scheme. Based on the invariant definition of the

divergence, we can derive a discrete analog $\mathbf{div}_h$ of $\mathbf{div}$ such that

$$\begin{array}{rccc} \mathbf{div}_h: & \tilde{V}_h \times \tilde{V}_h & \to & V_h \\ & \tilde{\mathbf{v}}_h & \hookrightarrow & \mathbf{div}_h\, \tilde{\mathbf{v}}_h, \end{array}$$

where $\tilde{\mathbf{v}}_h \equiv (\tilde{v}_h^x, \tilde{v}_h^y)$. Both $\tilde{V}_h$ and V_h are finite-dimensional spaces of discrete functions defined on the nodes and the cell-centers of Ω_h, respectively. Hence, the expression of the discrete divergence acting on a semidiscrete vector $\tilde{\mathbf{w}}_h(t)$ has the following form

$$\begin{aligned} (\mathbf{div}_h\, \tilde{\mathbf{w}}_h(t))_{i,j} = \frac{1}{2\sigma_{i,j}} & (((\tilde{w}_h^x)_{i+1,j+1} - (\tilde{w}_h^x)_{i,j})(\tilde{y}_{i,j+1} - \tilde{y}_{i+1,j}) \\ & -((\tilde{w}_h^x)_{i,j+1} - (\tilde{w}_h^x)_{i+1,j})(\tilde{y}_{i+1,j+1} - \tilde{y}_{i,j}) \\ & -((\tilde{w}_h^y)_{i+1,j+1} - (\tilde{w}_h^y)_{i,j})(\tilde{x}_{i,j+1} - \tilde{x}_{i+1,j}) \\ & -((\tilde{w}_h^y)_{i,j+1} - (\tilde{w}_h^y)_{i+1,j})(\tilde{x}_{i+1,j+1} - \tilde{x}_{i,j})), \end{aligned} \tag{2}$$

for $i \in \{1, 2, \ldots, N_x - 1\}$ and $j \in \{1, 2, \ldots, N_y - 1\}$, where $\sigma_{i,j}$ is the area of the (i,j)-cell and $(\tilde{w}_h^z)_{i,j}$ denotes the $((i-1)(N_y-1)+j)$-th component of $\tilde{w}_h^z(t)$ which approximates $w^z(x_{i,j}, y_{i,j}, t)$ for $z = x, y$.

Considering a discrete version of Gauss' theorem, together with equation (2), we shall construct the *derived operator* $\mathbf{gr\tilde{a}d}_h$ as the discrete analog of $\mathbf{grad}$ as follows

$$\begin{array}{rccc} \mathbf{gr\tilde{a}d}_h: & V_h & \to & \tilde{V}_h \times \tilde{V}_h \\ & u_h & \hookrightarrow & \mathbf{gr\tilde{a}d}_h\, u_h. \end{array}$$

The components of the discrete gradient acting on the semidiscrete function $\psi_h(t)$ can be obtained as

$$\begin{aligned} (\mathbf{gr\tilde{a}d}_h^x\, \psi_h(t))_{i,j} = \frac{1}{2\eta_{i,j}} & ((\tilde{y}_{i,j+1} - \tilde{y}_{i+1,j})\,(\psi_h)_{i,j} + (\tilde{y}_{i-1,j} - \tilde{y}_{i,j+1})\,(\psi_h)_{i-1,j} \\ & +(\tilde{y}_{i+1,j} - \tilde{y}_{i,j-1})\,(\psi_h)_{i,j-1} + (\tilde{y}_{i,j-1} - \tilde{y}_{i-1,j})\,(\psi_h)_{i-1,j-1}), \\ (\mathbf{gr\tilde{a}d}_h^y\, \psi_h(t))_{i,j} = \frac{1}{2\eta_{i,j}} & ((\tilde{x}_{i,j+1} - \tilde{x}_{i+1,j})\,(\psi_h)_{i,j} + (\tilde{x}_{i-1,j} - \tilde{x}_{i,j+1})\,(\psi_h)_{i-1,j} \\ & +(\tilde{x}_{i+1,j} - \tilde{x}_{i,j-1})\,(\psi_h)_{i,j-1} + (\tilde{x}_{i,j-1} - \tilde{x}_{i-1,j})\,(\psi_h)_{i-1,j-1}), \end{aligned} \tag{3}$$

for the internal values $i \in \{2, \ldots, N_x - 1\}$ and $j \in \{2, \ldots, N_y - 1\}$, where $\eta_{i,j} = 0.25\,(\sigma_{i,j} + \sigma_{i-1,j} + \sigma_{i,j-1} + \sigma_{i-1,j-1})$ and $(\psi_h)_{i,j}$ denotes the $((i-1)(N_y-1)+j)$-th component of $\psi_h(t)$ which approximates $\psi(x_{i,j}, y_{i,j}, t)$. It is easy to see that the previous equations can be extended to the boundaries if we introduce the following fictitious nodes

$$\begin{array}{llll} \tilde{x}_{i,0} = \tilde{x}_{i,1}, & \tilde{y}_{i,0} = \tilde{y}_{i,1}, & \tilde{x}_{i,N_y+1} = \tilde{x}_{i,N_y}, & \tilde{y}_{i,N_y+1} = \tilde{y}_{i,N_y}, \\ \tilde{x}_{0,j} = \tilde{x}_{1,j}, & \tilde{y}_{0,j} = \tilde{y}_{1,j}, & \tilde{x}_{N_x+1,j} = \tilde{x}_{N_x,j}, & \tilde{y}_{N_x+1,j} = \tilde{y}_{N_x,j}, \end{array}$$

for $i \in \{1, 2, \ldots, N_x\}$ and $j \in \{1, 2, \ldots, N_y\}$, as well as the evaluations of the Dirichlet boundary condition $\psi_D(\mathbf{x}, t)$ at the centers of the boundary segments, *i.e.*

$$(\psi_h)_{0,j} = \psi_D(\hat{x}_{1,j}, \hat{y}_{1,j}, t), \qquad (\psi_h)_{N_x,j} = \psi_D(\hat{x}_{N_x,j}, \hat{y}_{N_x,j}, t),$$

where $\hat{x}_{1,j} = 0.5\,(\tilde{x}_{1,j} + \tilde{x}_{1,j+1})$, $\hat{y}_{1,j} = 0.5\,(\tilde{y}_{1,j} + \tilde{y}_{1,j+1})$, $\hat{x}_{N_x,j} = 0.5\,(\tilde{x}_{N_x,j} + \tilde{x}_{N_x,j+1})$ and $\hat{y}_{N_x,j} = 0.5\,(\tilde{y}_{N_x,j} + \tilde{y}_{N_x,j+1})$, for $j \in \{1, 2, \ldots, N_y - 1\}$, and

$$(\psi_h)_{i,0} = \psi_D(\hat{x}_{i,1}, \hat{y}_{i,1}, t), \qquad (\psi_h)_{i,N_y} = \psi_D(\hat{x}_{i,N_y}, \hat{y}_{i,N_y}, t),$$

where $\hat{x}_{i,1} = 0.5\,(\tilde{x}_{i,1} + \tilde{x}_{i+1,1})$, $\hat{y}_{i,1} = 0.5\,(\tilde{y}_{i,1} + \tilde{y}_{i+1,1})$, $\hat{x}_{i,N_y} = 0.5\,(\tilde{x}_{i,N_y} + \tilde{x}_{i+1,N_y})$ and $\hat{y}_{i,N_y} = 0.5\,(\tilde{y}_{i,N_y} + \tilde{y}_{i+1,N_y})$, for $i \in \{1, 2, \ldots, N_x - 1\}$.

Let us next proceed to explain the spatial discretization for tensor $K(\psi)$. In the linear case studied in [9] (*i.e.* when $K \equiv K(\mathbf{x})$ does not depend on ψ), the discrete equations (3) together with the nodal evaluations of the components of K, denoted by $(\tilde{K}_h^{11})_{i,j}$, $(\tilde{K}_h^{12})_{i,j}$ and $(\tilde{K}_h^{22})_{i,j}$, lead us to

$$(\tilde{K}_h\,\mathbf{grad}_h\,\psi_h(t))_{i,j} = \begin{pmatrix} (\tilde{K}_h^{11})_{i,j}\,(\mathbf{grad}_h^x\,\psi_h(t))_{i,j} + (\tilde{K}_h^{12})_{i,j}\,(\mathbf{grad}_h^y\,\psi_h(t))_{i,j} \\ (\tilde{K}_h^{12})_{i,j}\,(\mathbf{grad}_h^x\,\psi_h(t))_{i,j} + (\tilde{K}_h^{22})_{i,j}\,(\mathbf{grad}_h^y\,\psi_h(t))_{i,j} \end{pmatrix}. \tag{4}$$

Now, using (2)-(4), it is straightforward to obtain the discrete linear operator $\mathbf{div}_h(\tilde{K}_h\,\mathbf{grad}_h)$. In this case, the local stencil for $(\mathbf{div}_h(\tilde{K}_h\,\mathbf{grad}_h\,\psi_h))_{i,j}$ involves the cell-centered approximations $(\psi_h)_{i-1,j-1}$, $(\psi_h)_{i,j-1}$, $(\psi_h)_{i+1,j-1}$, $(\psi_h)_{i-1,j}$, $(\psi_h)_{i,j}$, $(\psi_h)_{i+1,j}$, $(\psi_h)_{i-1,j+1}$, $(\psi_h)_{i,j+1}$ and $(\psi_h)_{i+1,j+1}$, as well as the evaluations of the components of K at the nodes (i,j), $(i+1,j)$, $(i,j+1)$ and $(i+1,j+1)$.

In the nonlinear case, the nodal discretization of $K(\psi)\,\mathbf{grad}\,\psi$ is similar to the one given by (4). However, as the conductiviy tensor depends on the unknown ψ, its discrete analog will involve approximations of such unknown at the grid nodes. Let us denote these approximations by $\tilde{\psi}_h$. Now, combining such discretization with equations (2) and (3), we shall obtain an approximation for $\mathbf{div}(K(\psi)\,\mathbf{grad}\,\psi)$. The local stencil for $(\mathbf{div}_h(\tilde{K}_h(\tilde{\psi}_h)\,\mathbf{grad}_h\,\psi_h))_{i,j}$ involves, as in the linear case, the cell-centered approximations $(\psi_h)_{i-1,j-1}$, $(\psi_h)_{i,j-1}$, $(\psi_h)_{i+1,j-1}$, $(\psi_h)_{i-1,j}$, $(\psi_h)_{i,j}$, $(\psi_h)_{i+1,j}$, $(\psi_h)_{i-1,j+1}$, $(\psi_h)_{i,j+1}$ and $(\psi_h)_{i+1,j+1}$; moreover, it includes the nodal approximations given by $(\tilde{\psi}_h)_{i,j}$, $(\tilde{\psi}_h)_{i+1,j}$, $(\tilde{\psi}_h)_{i,j+1}$ and $(\tilde{\psi}_h)_{i+1,j+1}$. Such values will be obtained by means of a bivariate interpolation method as linear combinations of the nine values of $\psi_h(t)$ at the cell centers, *i.e.*

$$(\tilde{\psi}_h)_{i,j} = \sum_{k,\ell=-1}^{1} c_{k,\ell}^{i,j}\,(\psi_h)_{i+k,j+\ell}, \qquad (\tilde{\psi}_h)_{i+1,j} = \sum_{k,\ell=-1}^{1} c_{k,\ell}^{i+1,j}\,(\psi_h)_{i+k,j+\ell},$$

$$(\tilde{\psi}_h)_{i,j+1} = \sum_{k,\ell=-1}^{1} c_{k,\ell}^{i,j+1}\,(\psi_h)_{i+k,j+\ell}, \quad (\tilde{\psi}_h)_{i+1,j+1} = \sum_{k,\ell=-1}^{1} c_{k,\ell}^{i+1,j+1}\,(\psi_h)_{i+k,j+\ell}.$$

Figure 1 shows the structure of the local nine-cell stencil corresponding to $(\mathbf{div}_h(\tilde{K}_h(\psi_h)\,\mathbf{grad}_h\,\psi_h))_{i,j}$.

Using this discretization for the diffusion term, we can approach the original problem by solving a nonlinear stiff initial-value problem of the form: Find ψ_h :

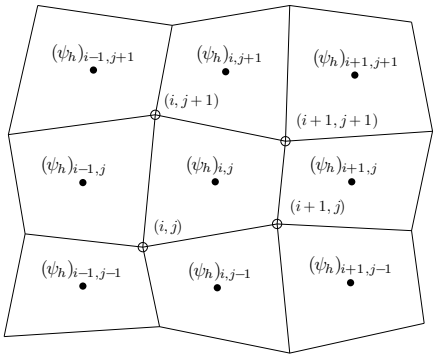

Fig. 1. Nine-cell stencil for $(\mathbf{div}_h(\tilde{K}_h(\psi_h)\,\mathbf{gr\tilde{a}d}_h\,\psi_h))_{i,j}$.

$[0,T] \to V_h$ such that

$$\begin{cases} \dfrac{d\psi_h(t)}{dt} = \mathbf{div}_h(\tilde{K}_h(\psi_h)\,\mathbf{gr\tilde{a}d}_h\,\psi_h(t)) + g_h(\psi_h) + f_h(t), \quad t \in (0,T], \\ \psi_h(0) = \mathbf{r}_h(\psi_0) = \psi_{0h}, \end{cases} \tag{5}$$

where $\mathbf{r}_h$ denotes the restriction to the cell centers of Ω_h.

3 Time Integration

Let us consider Ω decomposed into the union of m overlapping subdomains, where each one of them consists of a certain number of disjoint connected components, *i.e.*

$$\Omega = \bigcup_{i=1}^{m} \Omega_i, \text{ where } \Omega_i = \bigcup_{j=1}^{m_i} \Omega_{ij} \text{ such that } \Omega_{ij} \cap \Omega_{ik} = \emptyset \text{ if } j \neq k.$$

Next, we define a smooth partition of unity consisting of m functions $\{\rho_i(\mathbf{x})\}_{i=1}^{m}$, where each function $\rho_i : \Omega \to [0,1]$ is defined as follows

$$\rho_i(\mathbf{x}) = \begin{cases} 0, & \text{if } \mathbf{x} \in \Omega \setminus \Omega_i, \\ h_i(\mathbf{x}), & \text{if } \mathbf{x} \in \bigcup\limits_{\substack{j=1 \\ j \neq i}}^{m} (\Omega_i \cap \Omega_j), \\ 1, & \text{if } \mathbf{x} \in \Omega_i \setminus \bigcup\limits_{\substack{j=1 \\ j \neq i}}^{m} (\Omega_i \cap \Omega_j), \end{cases}$$

for $0 \leq h_i(\mathbf{x}) \leq 1$ and $\sum_{i=1}^{m} h_i(\mathbf{x}) = 1 \ \forall \ \mathbf{x} \in \bigcup_{\substack{j=1 \\ j \neq i}}^{m} (\Omega_i \cap \Omega_j)$.

By using this partition of unity, we shall define the following splittings for the nonlinear discrete operator $\mathbf{A}_h(\cdot) \equiv \mathbf{div}_h(\tilde{K}_h(\cdot)\,\mathbf{gr\tilde{a}d}_h\,\cdot)$ and the semidiscrete function $f_h(t)$ (*cf.* [3])

$$\mathbf{A}_h(\cdot) = \sum_{i=1}^{m} \mathbf{A}_{i,h}(\cdot), \qquad f_h(t) = \sum_{i=1}^{m} f_{i,h}(t). \tag{6}$$

Here, we denote $\mathbf{A}_{i,h}(\cdot) \equiv \mathbf{div}_h(\tilde{K}_{i,h}(\cdot)\,\mathbf{gr\tilde{a}d}_h\,\cdot)$, considering $\tilde{K}_{i,h}(\psi_h)\,\mathbf{gr\tilde{a}d}_h\,\psi_h$ as the discretization of $K_i(\mathbf{x},\psi)\,\mathbf{grad}\,\psi$, where $K_i(\mathbf{x},\psi) \equiv \rho_i(\mathbf{x})K(\psi)$. On the other hand, $f_{i,h}(t) \equiv \mathbf{r}_h(\rho_i(\mathbf{x})\,f(\mathbf{x},t))$.

Considering the splittings given by (6), the variant of the fractional implicit Euler method with m internal stages introduced in [1] reduces the nonlinear stiff problem (5) to the following set of nonlinear systems (one per internal stage)

$$\begin{cases} \psi_{h,0} = \psi_{0h}, \\ \psi_{h,n}^{k} = \psi_{h,n} + \tau \sum_{\ell=1}^{k} \left(\mathbf{A}_{\ell,h}(\psi_{h,n}^{\ell}) + f_{\ell,h}(t_{n+1})\right) + \tau\, g_h(\psi_{h,n}), \\ \qquad \text{for } k \in \{1,2,\ldots,m\}, \\ \psi_{h,n+1} = \psi_{h,n}^{m}, \\ \qquad \text{for } n \in \{0,1,\ldots,N_T\}, \end{cases} \tag{7}$$

where $N_T \equiv [T/\tau] - 1$. The discrete solution $\psi_{h,n+1}$ approximates $\psi_h(t_{n+1})$, where $t_{n+1} = (n+1)\,\tau$ and τ denotes the constant time step. The choice of the fractional implicit Euler scheme is motivated by the fact that this method is stable even when combined with an operator splitting which considers an arbitrary number of terms that do not necessarily commute (*cf.* [4]). This is the case for the discrete operators $\mathbf{A}_{i,h}(\cdot)$ involved in (6). Note that (7) also entails an explicit treatment of the nonlinear discrete function $g_h(\psi_{h,n})$.

In order to linearize (7), we approximate $\mathbf{A}_{\ell,h}(\psi_{h,n}^{\ell})$ by the two first terms of its Taylor expansion around $\psi_{h,n}$, *i.e.*

$$\mathbf{A}_{\ell,h}(\psi_{h,n}^{\ell}) \approx \mathbf{A}_{\ell,h}(\psi_{h,n}) + \left.\frac{d\mathbf{A}_{\ell,h}(\psi_h)}{d\psi_h}\right|_{\psi_h=\psi_{h,n}} (\psi_{h,n}^{\ell} - \psi_{h,n}). \tag{8}$$

If we denote by $(\psi_{h,n})_{i,j}$ the $((i-1)(N_y-1)+j)$-th component of $\psi_{h,n}$, for $i \in \{1,2,\ldots,N_x-1\}$ and $j \in \{1,2,\ldots,N_y-1\}$, then $(\mathbf{A}_{\ell,h}(\psi_{h,n}))_{i,j}$ depends nonlinearly on nine unknowns: $(\psi_{h,n})_{i-1,j-1}$, $(\psi_{h,n})_{i,j-1}$, $(\psi_{h,n})_{i+1,j-1}$, $(\psi_{h,n})_{i-1,j}$, $(\psi_{h,n})_{i,j}$, $(\psi_{h,n})_{i+1,j}$, $(\psi_{h,n})_{i-1,j+1}$, $(\psi_{h,n})_{i,j+1}$ and $(\psi_{h,n})_{i+1,j+1}$. Therefore, the $((i-1)(N_y-1)+j)$-th row of the Jacobian matrix $\mathbf{J}_{\ell,h}(\psi_{h,n}) \equiv d\mathbf{A}_{\ell,h}(\psi_h)/d\psi_h|_{\psi_h=\psi_{h,n}}$ will contain nine non-zero elements representing the derivatives of $(\mathbf{A}_{\ell,h}(\psi_{h,n}))_{i,j}$ with respect to each one of the previous unknowns.

Inserting (8) into (7), we obtain the totally discrete scheme for problem (1)

$$\begin{cases} \check{\psi}_{h,0} = \psi_{0h}, \\ \left(\mathbf{I} - \tau\, \mathbf{J}_{k,h}(\check{\psi}_{h,n})\right) \check{\psi}^{k}_{h,n} = \check{\psi}_{h,n} + \tau \displaystyle\sum_{\ell=1}^{k-1} \left(\mathbf{A}_{\ell,h}(\check{\psi}_{h,n}) + \mathbf{J}_{\ell,h}(\check{\psi}_{h,n})(\check{\psi}^{\ell}_{h,n} - \check{\psi}_{h,n})\right. \\ \qquad \left. + f_{\ell,h}(t_{n+1})\right) + \tau \left(\mathbf{A}_{k,h}(\check{\psi}_{h,n}) - \mathbf{J}_{k,h}(\check{\psi}_{h,n})\, \check{\psi}_{h,n} + f_{k,h}(t_{n+1})\right) + \tau g_h(\check{\psi}_{h,n}), \\ \qquad \text{for } k \in \{1, 2, \ldots, m\}, \\ \check{\psi}_{h,n+1} = \check{\psi}^{m}_{h,n}, \\ \qquad \text{for } n \in \{0, 1, \ldots, N_T\}, \end{cases} \tag{9}$$

where $\check{\psi}_{h,n+1}$ is an approximation of $\psi_h(t_{n+1})$ which preserves the same order of accuracy as $\psi_{h,n+1}$. Note that the domain decomposition splitting chosen for $\mathbf{A}_h(\cdot)$ makes each internal stage consist of a linear system which involves the unknowns lying just on one of the subdomains $\{\Omega_i\}_{i=1}^{m}$. Moreover, since each subdomain Ω_i comprises m_i disjoint connected components, this system can be immediately decomposed into m_i uncoupled subsystems which allow a straightforward parallelization. For those points lying outside subdomain Ω_i, we have that $\mathbf{J}_{i,h}(\check{\psi}_{h,n}) \equiv 0$ (remember that $\rho_i(\mathbf{x}) = 0$ if $\mathbf{x} \in \Omega \setminus \Omega_i$) and so, in this case, the solution of the i-th internal stage in (9) simply requires an explicit evaluation of the right-hand side. As a difference with respect to classical domain decomposition methods, artificial boundary conditions are not required on each subdomain and, hence, no Schwarz iterative procedures are needed in the computation. Finally, the uncoupled linear subsystems arising at each internal stage are solved by the Gauss-Seidel method.

In the case when $K(\psi)$ is a diagonal tensor and Ω is a rectangular domain discretized by means of a rectangular grid Ω_h, we can derive efficient algorithms for the solution of (1) by combining a finite difference spatial discretization with the time integration procedure described in this section. In such a case, we have two options for decomposing operator $\mathbf{A}_h(\cdot)$: the domain decomposition splitting explained before or a classical alternating direction splitting (*cf.* [1]). In the latter type, we obtain an essentially one-dimensional linear system at each internal stage which is tridiagonal and can be easily decomposed into several subsystems whose solution may be parallelized.

4 Numerical Experiment

In this section, we test the behaviour of the numerical algorithm on a set of pseudo-random logically rectangular grids. A similar test is shown in [8] for a classical implicit Euler scheme, combined with the support-operator technique, in the solution of linear parabolic problems.

Let us consider an equation of type (1) posed on $\Omega \times (0, T] \equiv \{\mathbf{x} = (x, y) \in \mathbb{R}^2 : 0 < x < 1,\ 0 < y < 1\} \times (0, 0.01]$. The hydraulic conductivity $K(\psi)$

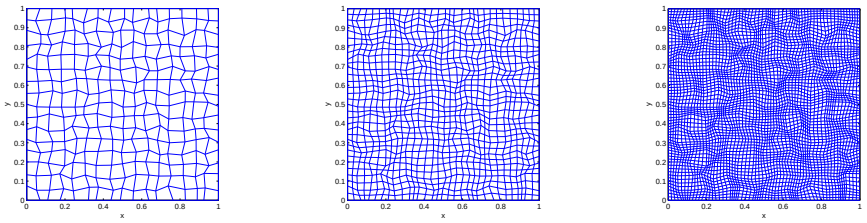

(a) $N = 17$ (b) $N = 33$ (c) $N = 65$

Fig. 2. Pseudo-random logically rectangular grids described in the numerical experiment.

is a full nonlinear tensor defined as $K(\psi) = Q(\theta)\, D(\psi)\, Q(\theta)^T$, where $Q(\theta)$ is a 2×2 rotation matrix with angle $\theta = \pi/4$ and $D(\psi)$ is a 2×2 diagonal matrix whose diagonal entries are $1 + \psi^2$ and $1 + 8\psi^2$. The nonlinear function is chosen to be $g(\psi) = 1/(1 + \psi^3)$, whereas the source/sink term $f(x, y, t)$ and both initial and Dirichlet boundary conditions are defined in such a way that $\psi(x, y, t) = e^{-2\pi^2 t} \sin(\pi x) \sin(\pi y)$ is the exact solution of the problem.

The spatial semidiscretization is based on the finite difference method described in section 2. The flow domain Ω is first discretized by means of a pseudo-random logically rectangular grid $\Omega_h \equiv \{(x_{i,j}, y_{i,j})\}_{i,j=1}^{N}$ with coordinates $x_{i,j} = (i-1)\, h - 0.25\, h + 0.5\, h\, R_x$ and $y_{i,j} = (j-1)\, h - 0.25\, h + 0.5\, h\, R_y$, where $h = 1/(N-1)$ and R_x, R_y are random numbers generated on the interval $(0, 1)$. Figure 2(a) shows an example of such type of grids for $N = 17$. In order to study the asymptotic behaviour of the error, we successively refine the original pseudo-random grid by using the following procedure: starting from a given grid, we add the lines which connect, on each cell, the centers of the opposite sides. Figures 2(b) and 2(c) show the first two refinements for the grid displayed on Figure 2(a).

Let us now consider a decomposition of Ω into $m = 4$ overlapping subdomains $\{\Omega_i\}_{i=1}^{m}$, each of which consists of $m_i = 4$ disjoint connected components, for $i \in \{1, 2, 3, 4\}$. In particular, if we denote $I_1 \equiv \left(0, \frac{1}{4} + d\right] \cup \left[\frac{1}{2} - d, \frac{3}{4} + d\right]$ and $I_2 \equiv \left[\frac{1}{4} - d, \frac{1}{2} + d\right] \cup \left[\frac{3}{4} - d, 1\right)$, the four subdomains are given by $\Omega_1 \equiv I_1 \times I_1$, $\Omega_2 \equiv I_2 \times I_1$, $\Omega_3 \equiv I_1 \times I_2$ and $\Omega_4 \equiv I_2 \times I_2$. Note that the width of the overlapping regions is $2d$, where d is chosen to be $1/16$. Next, we define a smooth partition of unity consisting of four functions $\{\rho_i(\mathbf{x})\}_{i=1}^{4}$ which are related to the previous domain decomposition. For that purpose, we start by introducing

$$h(x, x_0, d) = \exp\left(d \exp(1/d) \log(2) \frac{\exp\left(\frac{-1}{x - x_0 + d}\right)}{x - x_0 - d} \right),$$

τ	$\tau_0 = 10^{-3}$	$\tau_0/2$	$\tau_0/4$	$\tau_0/8$	$\tau_0/16$	$\tau_0/32$
$E_{N,\tau}$	3.703 E-2	2.577 E-2	1.613 E-2	9.416 E-3	5.246 E-3	2.827 E-3
$p_{N,\tau}$	0.5230	0.6759	0.7766	0.8439	0.8919	–

Table 1. Global errors and numerical orders of convergence for $N = 129$.

N	17	33	65	129	257
$E_{N,\tau}$	5.312 E-3	1.922 E-3	4.693 E-4	1.167 E-4	2.893 E-5
$p_{N,\tau}$	1.4667	2.0340	2.0077	2.0122	–

Table 2. Global errors and numerical orders of convergence for $\tau = 10^{-7}$.

which is subsequently used to define the functions

$$i_1(x) = \begin{cases} 1, & \text{if } \ x \in \left[0, \frac{1}{4} - d\right] \cup \left[\frac{1}{2} + d, \frac{3}{4} - d\right], \\ 0, & \text{if } \ x \in \left[\frac{1}{4} + d, \frac{1}{2} - d\right] \cup \left[\frac{3}{4} + d, 1\right], \\ h(x, \alpha, d), & \text{if } \ x \in [\alpha - d, \alpha + d] \quad \text{with } \alpha = \frac{1}{4}, \frac{3}{4}, \\ 1 - h(x, \frac{1}{2}, d), & \text{if } \ x \in \left[\frac{1}{2} - d, \frac{1}{2} + d\right] \end{cases}$$

and $i_2(x) = 1 - i_1(x)$. Finally, if we consider suitable products of $i_1(x)$ and $i_2(x)$, we can construct the following non-negative $\mathcal{C}^\infty$-functions: $\rho_1(x, y) = i_1(x)\, i_1(y)$, $\rho_2(x, y) = i_2(x)\, i_1(y)$, $\rho_3(x, y) = i_1(x)\, i_2(y)$ and $\rho_4(x, y) = i_2(x)\, i_2(y)$.

In order to obtain the totally discrete scheme (9), we use the fractional step method given by (7), with four internal stages ($m = 4$), in combination with the linearization procedure described in (8). The solution of our numerical scheme provides vectors $\psi_{h,n} \in \mathbb{R}^{(N-1)\times(N-1)}$, for $n = 1, 2, \ldots, N_T + 1$, whose components are approximations to the exact solution $\psi(\mathbf{x}, t_n)$ at the cell centers of Ω_h. Due to the domain decomposition splitting considered for $\mathbf{A}_h(\cdot)$, the linear system obtained at each internal stage reduces to a set of four smaller uncoupled subsystems which can be easily solved in parallel. Therefore, the number of unknowns involved in the computation will decrease from $(N-1) \times (N-1)$ to a number between $n_1 \times n_1$ and $n_2 \times n_2$, where $n_1 = (N-1)(1/4 + d)$ and $n_2 = (N-1)(1/4 + 2d)$. From a practical point of view, as the amount of available processors gets increased, each subdomain can be decomposed into a greater number of disjoint components in order to reduce the actual execution time.

Finally, we include two tables which contain the global errors, $E_{N,\tau}$ (upper row), and numerical orders of convergence, $p_{N,\tau}$ (lower row), obtained for different values of N and τ when using the maximum norm in time and the L^2-norm in space, *i.e.* $\|\cdot\|_{L^\infty(0,T;L^2(\Omega))}$. The method shows unconditional convergence of first order in time (see Table 1) and second order in space (see Table 2).

References

1. A. Arrarás, J.C. Jorge. An alternating-direction finite difference method for three-dimensional flow in unsaturated porous media. Mathematical Modelling and Analysis (2005) 57–64.
2. M.A. Celia, E.T. Bouloutas, R.L. Zarba. A general mass-conservative numerical solution for the unsaturated flow equation. Water Resour. Res. 26 (1990) 1483–1496.
3. L. Portero, B. Bujanda, J.C. Jorge. A combined fractional step domain decomposition method for the numerical integration of parabolic problems. Lecture Notes in Comput. Sci. 3019 (2004) 1034–1041.
4. L. Portero. Fractional Step Runge-Kutta Methods for Multidimensional Evolutionary Problems with Time-Dependent Coefficients and Boundary Data. Ph.D. Thesis, Universidad Pública de Navarra, Pamplona, 2007.
5. L.A. Richards. Capillary conduction of liquids through porous mediums. Physics 1 (1931) 318–333.
6. A. Samarskiĭ, V. Tishkin, A. Favorskiĭ, M. Shashkov. Operational finite-difference schemes. Differ. Equ. 17 (1981) 854–862.
7. M. Shashkov. Conservative Finite-Difference Methods on General Grids. CRC Press, Boca Raton, 1996.
8. M. Shashkov, S. Steinberg. Solving diffusion equations with rough coefficients in rough grids. J. Comput. Phys. 129 (1996) 383–405.
9. M. Shashkov, S. Steinberg. The numerical solution of diffusion problems in strongly heterogeneous non-isotropic materials. J. Comput. Phys. 132 (1997) 130–148.
10. J. Šimůnek, J.W. Hopmans, J.A. Vrugt, M.T. van Wijt. One-, two- and three-dimensional root water uptake functions for transient modeling. Water Resour. Res. 37 (2001) 2457–2470.